

Personalized Hip Replacement: State of the Art and New Tools Proposals

Isabel Moscol¹^a, William Solórzano-Requejo^{1,2}^b, Carlos Ojeda¹^c and Ciro Rodríguez³^d

¹Department of Mechanical and Electrical Engineering, Universidad de Piura, Piura, Peru

²ETSI Industriales, Universidad Politécnica de Madrid, Madrid, Spain

³Department of Software Engineering, Universidad Nacional Mayor de San Marcos, Lima, Peru

Keywords: Hip Arthroplasty, Biomaterials, Short Stems, FEA Software, Artificial Intelligence.

Abstract: Hip replacement is one of the most successful surgical events that progressively more patients require because of the better life expectancy and increase in the average age of several countries. It further promoted the improvement of hip prosthesis lifespan in sciences such as materials, mechanics and, recently, computer science with artificial intelligence (AI). The present investigation aims to make a systematic review of the progress with recent developments and criteria to get optimal outcomes in the design and selection of hip implants, emphasizing femoral stem parameters for their relevance to the entire prosthesis performance. New software tools such as clustering, and a different finite element analysis (FEA) approach are introduced to speed up customized design processes without sacrificing accuracy. Clustering algorithms delimited the proximal femur properly according to its anatomical locations. Moreover, Altair SimSolid[®] software proved satisfactory accuracy compared to NX[®] simulation values despite the complex morphology of the proximal femur with a maximum deviation of 12.94% and a simulation time of less than 30%.

1 INTRODUCTION

One of the main and largest joints in the human body is the hip. It constituted by the femoral head and the acetabulum through the articular cartilage, acetabular labrum and ligaments. Moreover, the femur is the longest and heaviest bone, receives and physiologically distributes the gravitational loads of the body. Different conditions such as walking, jogging, sitting, among others accentuate the loads, so it requires high resistance; however, the arrangement of the hip joint ensures a proper physiological transfer of loads enabling stability and mobility at the same time.

Total hip arthroplasty is one of the most successful surgical procedures (Learmonth et al., 2007). It has undergone extensive development (Figure 1) due to its high demand because increasingly younger patients require a hip

replacement, and also, in several countries, the population is getting older.

This surgical procedure is performed when non-invasive treatments fail to relieve pain or restore mobility in the patient's hip. It mainly occurs when there is a femoral neck fracture, intertrochanteric fracture, coxarthrosis, or other pathology associated with the hip joint, often linked to low bone quality or cartilage degradation. Demand for a primary total hip replacement among people less than 65 years old was projected to exceed 52% by 2030 (Kurtz et al., 2010). In young patients, hip fracture risk appears when extremely high loads are transferred usually in a short time due to accidents.

Hip replacement removes the damaged parts of the femur and acetabulum to replace them with artificial limbs named hip prosthesis, whose components are the cup, insert, femoral head, and stem. The latter has a crucial function in the success

^a <https://orcid.org/0000-0001-8959-9547>

^b <https://orcid.org/0000-0002-2989-9166>

^c <https://orcid.org/0000-0001-6163-5382>

^d <https://orcid.org/0000-0003-2112-1349>

and duration of the implant since it will be in direct or indirect (through cement) contact with the femoral cavity, being in charge of proper load transferring to the proximal femur. The objective is to make this transfer as close as possible to the natural biomechanical behaviour by the optimal design and fixation.

Despite the technological advances, there are still several postoperative pathologies related to multiple incompatibilities caused by the external agent. Corrosion and wear debris, associated with biomaterial properties, are responsible for osteolysis inducing bone inflammation and resorption that eventually lead to periprosthetic loosening of the implant (Eltit et al., 2019). Moreover, differences in mechanical properties promote Stress/Strain Shielding (SS) because of Young's modulus variation between implant and bone (Table 1), this phenomenon promotes bone resorption on the periprosthetic region of the stem.

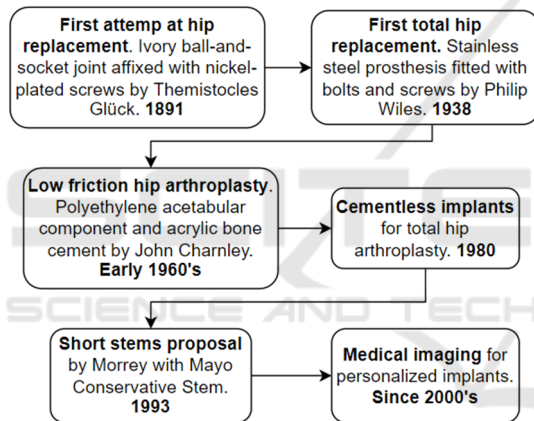


Figure 1: The temporal sequence of hip prostheses.

In the last two decades, development in computational tools like CAD/CAE software and AI have been valuable tools for more accurate and time-optimized experimentation. Many design and selection processes could now be automated so that orthopaedic physicians or biomedical engineers save time and reduce the number of possible solutions to evaluate.

These tools can improve surgical outcomes by ensuring precision in several parameters such as the positional coordinates and forces to ensure adequate initial fixation of the implant. Robotic hip surgery was initiated in the 1980s with the DigiMatch Robodoc surgical system produced by the company then called Integrated Surgical Systems (Subramanian et al., 2019). This system helps preoperative planning in which patient's Computed

Tomography (CT) guides the surgeon in the implant selection and previews the postoperative outcomes. Nowadays, there've been several improvements and another part of the Robodoc performs the osteotomy bone cut and inserts the implant minimizing human error and the risk of bone fracture during the surgery (Sugano, 2013).

2 TYPES OF HIP PROSTHESES

In 1959, Sir John Charnley proposed the *low friction* total hip arthroplasty where a small-diameter socket restores the total mobility of the joint and eradicates pain. Despite the good technical skills of the surgeons, there were still several failure cases. For that reason, in 1962 Craven suggested the high-density polyethylene (HMWP) as a material for the socket that was an excellent complement for Charnley's design proposal. (Camacho & Fernandez, 2006)(Wroblewski, 1997). However, the failure rate of the Charnley prosthesis was higher in young patients, who are estimated to lead more physical activity moving their hip around 5 million cycles per year (Gallart et al., 2018). To recover the entire mobility and mechanical demands, the cement goes under high mechanical stresses which, in most cases, led to its fracture.

Moreover, outcomes of cement fixation are not the same for patients with good bone quality as in patients with greater porosity. Better cement-bone bond is achieved when the patient has a less bone mass index. (Learmonth et al., 2007)(Cotogno, 2012).

This controversy promoted the introduction of cementless fixation in 1980, whose target is to guarantee long-term biological stability through bone ingrowth on the stem walls, a process known as osseointegration. It results from direct bone-implant contact with biocompatible porous coating and minimal interface micromotion (Nazari-farsani, 2015). Relative displacements are related to surgical technique, implant geometry and stiffness, bone quality, daily activities, and patient weight. The appropriate geometry would enhance primary/mechanical stability within 3 to 6 months after surgery and the good engagement of the prosthesis with the surrounding bone lead to secondary/biological one due to good osseointegration (Javed et al., 2013)(Ruben et al., 2007). The proper implant would have a high rate of success if the patient's bone remodelling was also good, that is why these types of implants are recommended for young patients.

Although cementless fixation showed remarkable designs continued to be invasive since they occupy from the proximal region to the upper part of the femoral diaphysis. It would lead to obstructing the bloodstream that provides oxygen and nutrients for bone maintenance. Reducing bone remotion in the surgical procedure and optimizing the load transfer, through appropriate implant geometry and material, would ensure bone preservation and a long prosthesis lifespan (Gallart et al., 2018).

A study by (Jasty et al., 1993) showed that the diaphyseal portion of the stem was rendered unusable when the bone grew proximally. Other studies about diaphyseal anchorage indicated it is associated with anomalous load transfer, leading to thigh pain in the short term and proximal bone loss by SS in the long term (Amstutz & Duff, 2015). Therefore, the need arises to shorten the stem length with designs that span to the metaphyseal region of the proximal femur, giving rise to the field of short-stem prostheses.

Short stems, also called metaphyseal stems, leave more bone stock available for being smaller. They could also preserve bone by distributing loads more physiologically. Recent studies show less bone mineral density loss in the proximal region for patients with this type of stem and a reduced proximal SS (Sköldenberg et al., 2006). Short stems have been classified by different authors according to their geometry and anatomical zones occupied in the proximal femur, resulting in four main categories:

- Type 1: Femoral neck stem.
- Type 2: Calcar loading stem.
- Type 3: Calcar loading with lateral flare stem.
- Type 4: Shortened tapered conventional stem.

Short stems usually have a length between 40 and 135 mm, reaching at most to the superior diaphysis as in the case of tapered-wedge designs. The best results according to literature are related to the calcar loading with lateral flare stems, whose tapered trapezoidal design achieved adequate fixation and demonstrated



Figure 2: Proximal femur occupied by the Type 3 short stem DePuy Proxima™ (Santori et al., 2007).

more effective load transfer in the proximal femur than the other designs (Khanuja et al., 2014)(Kheir et al., 2020).

Within the category of calcar short stems, load bearing with lateral flare designs have shown the highest rate of success. In this category, the DePuy Proxima™ (DePuy, Leeds, UK) model (Figure 2) is found standing out with overall survival of 100% for 4.5 years and 97.6% for 7 years according to follow-up studies made by (Kim et al., 2013) and (Gombár et al., 2019), respectively.

3 BIOMATERIALS

3.1 Importance and Influence

Biomaterials must meet several requirements that vary according to whether the prosthesis is cemented or uncemented. In the first category, usually, Polymethylmethacrylate (PMMA) cement will be in direct contact with the bone while, in the second, stem walls, normally covered by a porous material, will enable the stem fixation. Accordingly, biomaterials will vary depending on their function either in the body of the components or as a coating or bone cement. In general, the body/internal component material must be compatible with mechanical properties as close as possible to the bone; otherwise, stresses transmitted to the bone would be reduced to such an extent that SS occurs. To achieve this, good mechanical strength, as well as fatigue resistance are required.

Cemented fixation guarantees primary stability just after the bone cement has set due to the hardening properties of the cement which mechanically fixes and prevents relative mobility at the bone-implant interface. A homogeneous cement layer with a good setting improves mechanical fixation, contributing as well to the physiological transfer of loads and reducing SS (Cotogno, 2012). The cemented implant proposed by Sir John Charnley has a probability of success between 77% and 81% over a range of 25 years after THA, but the failure rate was higher for young patients. The first problem was related to the material of the acetabular component, polyethylene (PE), whose debris infected the bloodstream due to metallosis (Rieker, 2016)(Hu & Yoon, 2018). This material was then replaced by high-density polyethylene (UHMWPE, ultra-high molecular weight polyethylene). However, the rate of failure persisted because of incompatibilities between the bone cement, the active lifestyle, and bone quality of these patients.

A study made on 48 patients younger than 30 years with cemented hip implants showed a 10-year survival of 83% with revision for any reason and 90% with revision for aseptic loosening as the endpoint (Busch et al., 2010). A post-study (Schmitz et al., 2013) with the same population and revision criteria showed a 15-year survival rate of 75% and 82%, respectively. However, this option is more recommended for young people with degenerative cartilage disease in the hip joint and aseptic loosening is accompanied sporadically by aggressive bone destruction, a phenomenon termed *cement disease* (Barrack, 2000).

As a result, cementless prostheses were proposed to take advantage of the good bone quality that younger patients have. Implant success is highly correlated to initial stability which is essential to promote bone ingrowth into the stem coating (Ruben et al., 2012). The stem coating must enhance osseointegration and be resistant to wear and corrosion to minimize the release of particles into the bloodstream and avoid toxicity. Most of the implants commonly use a porous coating called Hydroxyapatite [$\text{Ca}_{10}(\text{PO}_4)_6(\text{OH})_2$] whose bioactive interaction accelerates the bone ingrowth process through a series of reactions between the biomaterial and the internal fluids of the femur that form a biologically active carbonate layer, equivalent to the bone mineral phase (Cotogno, 2012).

The primary stability is also related to stem geometry and materials that likewise influence biological stability where minimized stress shielding is required. One of the main factors about implant material is the stiffness level. Highly stiff implants induce less micromotion compared to low-stiff ones, nonetheless, high-stiff materials promote stress shielding and adverse bone remodelling at the implant surfaces (Chanda et al., 2020). The long-term stability of cementless prostheses also depends on the patient's health, especially bone quality, which influences on bone remodelling rate in the periprosthetic region.

3.2 New Materials

Several types of materials like ceramics, polymers and metals have been developed for implants purposes. They classify based on their interaction with the surrounding tissue in bio-tolerant, bioactive and bioresorbable. Metals have shown good quality outcomes being the most commonly used: stainless steel (316L), cobalt-based alloys (Co-Cr-Mo) and titanium-based alloys (Ti-6Al-4V, Ti-5Al-2.5Fe, Ti-Al-Nb) (Aherwar et al., 2016). Nowadays, titanium is the most used material in femoral stems manufacture,

it is characterized by low density, highly biocompatible with good resistance to stress and corrosion; the latter is since there is a rapid reaction with oxygen that generates a thin protective layer. Its alloys, especially Ti-6Al-4V, have shown good results in reducing SS by having a lower Young's modulus than other types of alloys; however, this is approximately 110 GPa, still high compared to cortical bone (Kunii et al., 2019) producing SS due to a disproportionate bone remodelling.

Prior biomechanical studies (Kuiper & Huiskes, 1996) concluded that decreasing stem stiffness reduces stress shielding and avoids severe bone resorption. Nevertheless, it increases proximal interface stresses, which may inhibit biological fixation and cause loosening.

A non-homogeneous Young's modulus material proposed in (Hanada et al., 2014) is β -Ti33.6Nb4Sn (TNS) obtained after several cold working and local heat treatments. It has high strength with Young's modulus (45 GPa with cold rolling) much lower than other β -type Titanium alloys: axial stiffness 56% lower and bending stiffness \leq 53% lower than Ti6Al4V (Yamako et al., 2017). In studies with TNS, a low Young's Modulus in the distal part of the stem and high fatigue strength (850MPa) in the neck region were proposed. However, rather low Young's modulus, although decreasing stiffness, could cause excessive stresses at the bone-implant interface inhibiting fixation; additionally in vivo studies must include adaptative bone remodelling to determine whether bone changes occur in the surrounding tissue. Despite that, studies show that bone mineral density would be 42.6% higher in the Gruen 7 zone with a TNS stem than Ti-6Al-4V 10 years after implant placement. Another new option is the Ti21S alloy (Pellizzari et al., 2020), whose biocompatibility is like Ti6Al4V, which generates more mechanical advantages by having Young's modulus of approximately half, as shown in Table 1.

Table 1: Mechanical properties of Titanium alloys for hip prostheses.

Alloy	Young's Modulus (GPa)	Tensile Strength (MPa)	Reference
Cortical Bone	10 - 20	100 - 300	(Cotogno, 2012)
Ti-33.6Nb-4Sn (TNS)	55	1270	(Yamako et al., 2014)
Ti-6Al-4V	110	1095	(Facchini et al., 2011)
β - Ti21S	52	831	(Pellizzari et al., 2020)

Recent studies are evaluating biomechanical properties obtained with additive manufacturing where adaptative cell topologies resemble bone local mechanical properties. In (Arabnejad et al., 2017) obtained a 75% reduction in bone loss derived from stress shielding (8% of bone resorption with the optimized fully porous implant) compared to a solid implant.

4 PERSONALIZED PROSTHESES

Hip implant longevity is increased by customizing the prosthesis design. This implies considering the offset, anteversion, and neck-shaft angle (Figure 3). Before starting the design and the implant material selection, it is necessary to know the host bone properties (Solórzano et al., 2020) and the patient’s health situation. This way, better performance outcomes and durability of the hip prostheses can be guaranteed.

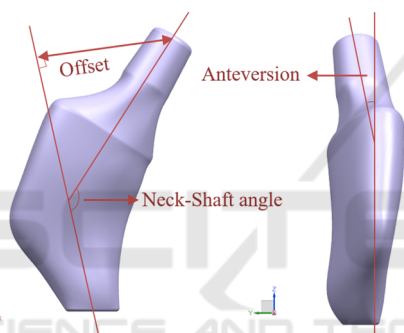


Figure 3: Femur parameters considered in a customized design.

The most noticeable physiological changes are due to the patient's age because, after a certain age, bone quality begins a noticeable decline attributed to metabolic changes in the bone tissue and a decrease in bone osteocalcin content (Portal-Núñez et al., 2012). Thus, if the patient is young, the hip joint will be subjected to higher mechanical loads and is more likely to undergo revision surgery compared to an older patient. Therefore, a less invasive stem will be required. Moreover, the more active bone tissue of young patients makes them suitable for the use of cementless prostheses, as it promotes osseointegration, which accelerates primary stability and increases implant life by forming a stronger bond than cemented fixation (Sivasankar et al., 2016).

Another way to customize hip prostheses was proposed in Milan around 1987 by Cremascoli (Srinivasan et al., 2012). He suggested the modular neck to give independence and adaptability according to physical attributes of the patient's joint, such as

offset, femoral neck anteversion, and neck length. Modular prosthesis presents two components (stem and neck separately) coupled by a taper junction with frictional bonding. The literature reveals no noticeable variation in the long-term outcomes of modular and non-modular prostheses; in contrast, adverse effects such as fretting corrosion and fatigue probably occur at the junction of modular prostheses (Kheir et al., 2020)(Schaaff, 2004).

Therefore, *monoblock* customization of the implants is recommended. It involves considering proximal and distal morphologies of the femur for more accurate stem personalization. In this regard, CT allows virtual reconstruction of a patient’s femur (Figure 4). Uncemented prostheses adapted to the inner part of the femur provide a better fit due to their optimized volume, which also reduces the weight of the implant. In this way, the stress distribution and biomechanics of the joint resemble its natural state (Katoozian et al., 2001).

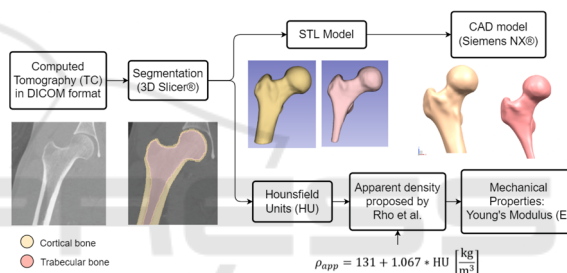


Figure 4: Femoral geometry and properties from computed tomography.

In 2009, (Ojeda, 2009) verified by numerical simulation the preponderance of customized prostheses. The study was performed with the computed tomography (CT) of a 40-year-old woman from Piura, Peru. Primary stability in a conventional cementless prosthesis was assessed through micro-displacements at the femur-stem interface. The custom design was superior to the CLS Spotorno® model, but the relative micromotion in the posterior lateral proximal zone remained high, ranging from 150 to 200 microns. It is therefore important to evaluate the lateral zone on the stem design.

The stem is crucial to improving prosthesis performance because it is subjected to the highest mechanical stresses and manage the physiological transfer of loads to the surrounding bone. Firstly, stem length affects the mechanical stability; hence the longer, the better. However, this implies greater invasion of the marrow cavity leaving less bone available for possible revision surgery. As a consequence, shorter stems are recommended for patients younger than 65 years (Cotogno, 2012). The

custom design of short stems is performed with the same methodology as conventional stems. However, load distribution along the femur should be taken into account, especially in the calcar and lateral regions of the proximal femur due to its preponderance to the SS. (Rawal et al., 2011)(Gómez-García et al., 2016). (Solórzano, 2021) evaluated by FEA personalized short stems with Ti21S material resulting in a SS of 0.285 and 0.073 for each of two patients; those prostheses would improve mechanical response and remodelling of the proximal femur than commercial hip implants (Yamako et al., 2014)(Yan et al., 2020) which could produce a SS between 0.61 and 0.93.

5 TECHNOLOGIES

5.1 Statistics and Artificial Intelligence in Hip Arthroplasty

Initially, statistical methods (Otomaru et al., 2012) introduced automation to segment the marrow cavity and ensure prosthesis implantability. They combined tolerance criteria of experienced surgeons and a map of distances at the bone-implant interface based on a set of medical images to create an atlas with the delimitation of the maximum areas within the channel cross-section where the stem geometry could be fitted.

Last decade, Artificial Intelligence has been progressively gaining more space in the healthcare field. In 2020, (Kang et al., 2020) applied Convolutional Neural Networks (CNNs) with X-Ray imaging to build a stem detection model to classify and cluster different commercial models. The algorithm could help to collect large-scale stem information and to make comparisons among different geometries which in the future would save time for orthopaedists to identify and make new selections among commercial prostheses.

Recently, Chitubox[®], a 3D printing software, allowed (Bermejillo et al., 2021) to slice CAD models obtaining a set of white and black pictures that resemble CT images. That methodology can be used in the design of femoral stems to acquire information not only from the stem but also from the medullary cavity. The slices of the proximal femur (Figure 5) would be used to train a CNN that predicts femoral response, like SS. Customization would be done by evaluating femur response changing the pixel status of stem portions. Then, after training AI models for optimization, it could be used with real CT scans to make personalized stems that restore bone biomechanics with ideal performance concerning physiological load transfer.

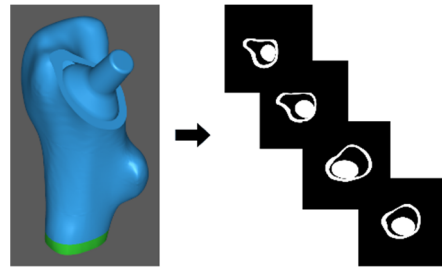


Figure 5: CT-like slices of a femur with hip replacement using Chitubox[®] software.

Advanced AI tools are required to make a more complete description of complex geometries. Moreover, ML-based methodologies may be applicable when the computational costs of numerical simulation are unaffordable. Several studies are underway to improve the performance of AI-based systems to streamline design processes with adequate accuracy.

The present investigation proposes clustering techniques (Figure 6) to make a more accurate and time-saving assessment of the proximal femur. It aims to get local information about the physiological load transfer according to femoral anatomical locations: lateral, medial, anterior, and posterior.

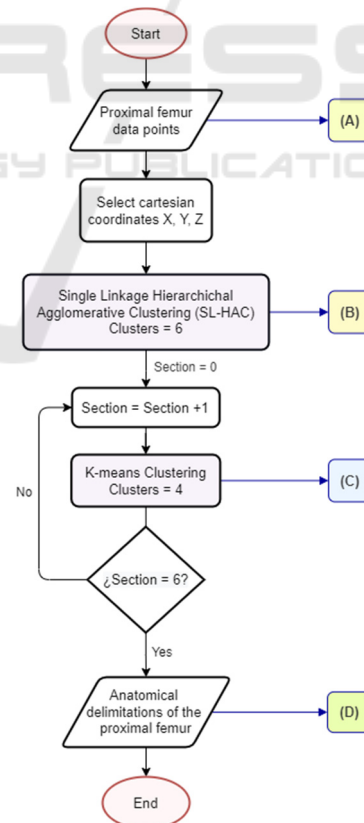


Figure 6: Flowchart to anatomically demarcate proximal femur.

The angular association among the proximal femur planes is based on (Solórzano, 2021) proposal of an innovative methodology for short stem designs that guarantees stem implantability by acquiring information of the medullary cavity and surgery approach. The first plane corresponds to the osteotomy plane taken from the CAD model of the proximal femur of the patient, whose CT scans were downloaded from an open-access medical image repository (Raymond, 2019). The second reference is a horizontal plane located 10mm below the lesser trochanter. Finally, with equal division of the osteotomy angle, six planes are obtained as is shown in Figure 7.

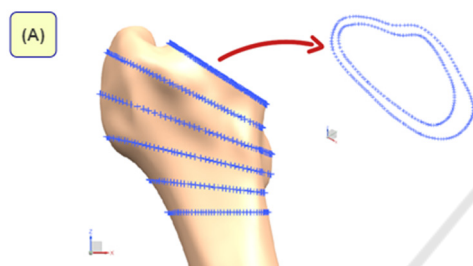


Figure 7: Cortical bone points to be classified.

Through the SL-HAC, bone sections can be identified without manually labelling each one (Figure 8). Initially, all samples are individual clusters, then the algorithm calculates the distance between the most similar for each pair of clusters to then combine those who are closer. This division allows working with points that contain not only rectangular coordinates but also the local femur response to mechanical stimuli in stress, strain, among others values.

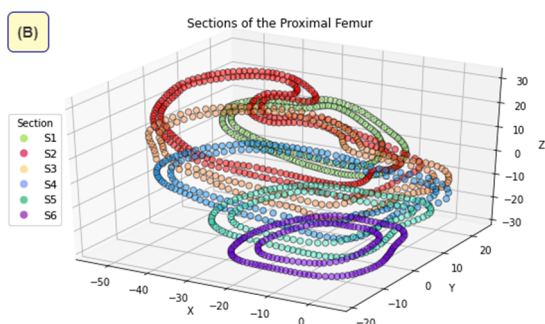


Figure 8: Sections generated by the SL-HAC algorithm.

The final clustering shown in Figure 9 is made automatically by a K-Means algorithm through an iterative update of the centroids, identified randomly at the beginning. This ML technique is good at

dealing with data of spherical distribution. Same K-Means specifications were applied to each of the six planes in Figure 7.

One of the main benefits of this approach relies on increasing ML-based models, where speeding up data acquisition with high accuracy is required. These delimitations (Figure 10) provide insight into changes in physiological load distribution and bone biomechanics as a function of varying load patterns. SS can also be quantified and analyzed in detail with this demarcation of the proximal femur.

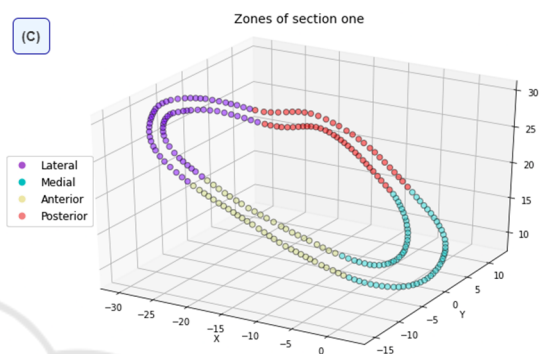


Figure 9: Zones of one section by K-Means algorithm.

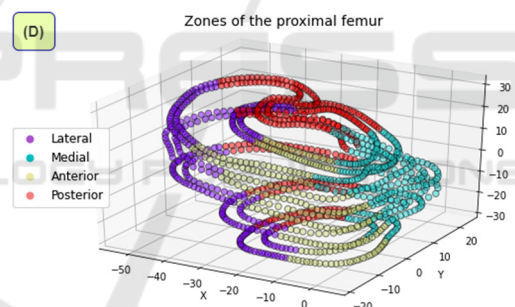


Figure 10: Proximal femur completely delimited according to the anatomical locations.

Regarding mechanical design, in 2015, (Chanda et al., 2015) designed an Artificial Neural Network to relate geometric parameters of the stem to micro-displacements at the bone-implant interface. They also included optimization through Genetic Algorithms (GA) to improve mechanical stability, but SS is not guaranteed due to its micromotion approach that doesn't quantify the loads received by the femur. In 2017, (Cilla et al., 2017) studied whether the geometry of a commercial femoral prosthesis could be effectively optimized to reduce the SS. They compared Support Vector Machines (SVM) and Artificial Neural Networks (ANNs) after combining them with Pattern Search minimization algorithm (Table 2). SVM gave better results; however, the

effectiveness may vary from patient to patient and depending on the amount of data.

A recent innovation regarding the improvement in optimization algorithms was raised in 2019, where (Chatterjee et al., 2019) introduced the concept of the composite desirability function to solve the problem of obtaining a single value as output from ANNs. This function made it possible to consider the susceptibility to significant stress variations in each proposed region after the prosthesis was placed. They also parameterized the patient's bone quality, quantifying its influence on the same problem.

Table 2: Algorithms for Design Optimization.

Algorithms	Highlights
To estimate the femur response to the supported loads	
Artificial Neural Networks (ANN)	Attempts to mimic the human brain for solving specific tasks finding complex associations among data like a black box.
Support Vector Machines (SVM)	SVM do not retrain the model to estimate a new value once it has already been trained and tested. It adds the new remark directly and updates itself.
To find the optimal geometry optimizing a cost function	
Genetic Algorithms (GA)	Stochastic global search method based on the Darwinian concept of survival. It uses the principle of natural selection and genetic inheritance by evaluating a fitness score.
Pattern Search (PS)	Numerical optimization method that computes objective function (OF) for the points in a grid. It explores more than it exploits by changing iteration with the first point exceeding the best OF.

5.2 FEA Software

Requirements of large amount of data have also turned attention to fast simulation software and to understanding how they work. In conventional analysis, simulation of a virtual femur could take from 5 to 15 minutes depending on computer specifications, the geometric complexity of the model and boundary conditions as well as the meshing characteristics.

Around 2018, a meshless software called SimSolid® from Altair Engineering Inc. was launched. It proposes a new FEA approach where no discretization in finite elements is done but takes any

type of geometry, whether simple, amorphous or complex such as the proximal femur and considers it as a *finite element* (FE) (Altair, 2019). Furthermore, this software works with contour functions that generate the degrees of freedom (DOF) of the FE/component, unlike the conventional approach where the number of nodes of the discretized finite element defines its DOF. In addition, the contour DOF are not the only ones produced when developing the external approximations in SimSolid®, but also the internal DOF associated with the volume are generated automatically. Meshless software performs adaptive solutions where the number of DOF of the boundary is automatically assigned to meet the convergence criteria.

Simulation time is another advantage of meshless simulation. For femoral analysis, SimSolid® takes from 30 seconds to 1 minute depending on default solution settings and it could take from 3 to 6 minutes with increased refinement level. In addition, not using meshing saves time for model pre-processing, whereas in conventional FEA simulation the element size must be defined according to h-method and p-method through convergence analysis.

The mathematical formulation of the meshless approach, specifically SimSolid®, dates to 1908 when Ritz proposed an approximate solution to the boundary value problem with the linear combination of simple functions (p_i). In (1), a_i are factors without physical representation defined when the energy function, $F(U_{h,element})$ in (2), is assigned to a minimum value, n is the number of nodes of the FE.

$$U_{h,element} = \sum a_i \cdot p_i, \quad \forall i = 1, 2, 3, \dots, n \quad (1)$$

$$F(U_{h,element}) = F(\sum a_i \cdot p_i) = \min \quad (2)$$

Equation (3) is satisfied for the FE approximation to be external of the element. \langle, \rangle refers to the pairs that lie on the element boundary. δ and γ are operators, U and are approximation functions defined inside the element. Altogether in (3) guarantees that the boundary of the limit approximation functions of U belong to the Sobolev space which guarantees their existence only to a certain degree so $F(U)$ provides finite energy. (SimSolid Corporation, 2015)

$$\langle \delta, \gamma U \rangle = 0 \quad (3)$$

In (4) boundary DOF are also defined, which have no physical meaning. Their function is to guarantee that the approximation functions (U) of each FE are compatible when B_{DOF} tends to infinity.

$$B_{DOF} = \int_{\gamma} g_k \gamma U d\gamma, \forall k = 1, 2, \dots, n \quad (4)$$

- γ : the boundary of the finite element.
- g_i : simple functions on the boundary of the FE.

In (3), U is the function to be approximated in the element like stresses or displacements in structural analysis. When it comes to external analysis, the U_h function from (5) and (6) not only incorporates the element but also considers its boundary.

$$U_h = U_{element} + U_{boundary} \quad (5)$$

$$U_h = \Sigma a_i(U)p_i + \Sigma \left(\int_{\gamma} g_k \gamma U d\gamma \right) p_k \quad (6)$$

In equation (6),

- a_i : internal DOF of the element.
- p_i : basis functions within the internal DOF.
- p_k : basis functions of the boundary DOF.

Literature shows that SimSolid® presents a deviation concerning other numerical simulation software lower than 1% in the high-stress concentration elements, reaching values lower than 5% in all cases (skew plate, plate with hole, U-shaped notch) with the maximum precision setting, reducing variation from 29.3% to 2.8% compared to the default configuration (Symington, 2020). The only study found with human geometry (Rivera et al., 2020) evaluated a mandible reconstructed from a CT scan getting 2-7% of deviation when compared with other FEA software.

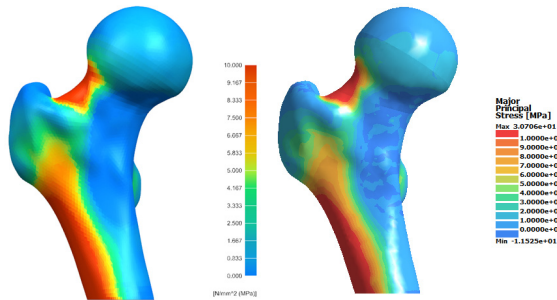


Figure 11: Maximum principal stresses of the intact femur under ISO load with NX® and SimSolid®.

Figure 11 shows simulation results with the following boundary conditions: rigid fixation at the bottom, adherence of cortical and trabecular bone contact surfaces and a 2300N force established by the International Standardization Organization (ISO) under the ISO 7206-4 standard.

Maximum Principal Stress is suggested for analyzing stress distribution in bones (Solórzano et al., 2020)(Jung & Kim, 2014)(Schileo et al., 2008). Likewise, Von Misses stress was considered due to its previous use as a reference to compare the accuracy of SimSolid® (Symington, 2020) even in a biomechanical study on the mandibular structure (Rivera et al., 2020). Von Misses stresses are also used to assess the implant fracture risk that in the proximal femur customization approach could have relatively complex geometries.

Table 3: Results comparison between both software.

	NX®	SimSolid®	Deviation
<i>Maximum Principal Stress</i>			
Maximum	35.270	30.706	12.94%
Minimum	-12.796	-11.525	9.93%
<i>Von Misses Stress</i>			
Maximum	30.482	30.740	0.85%
Minimum	0.033	0.036	9.09%

The maximum deviation was 12.94% and the rest were less than 10%, which is acceptable if we deal with a complex morphology such as a femur (Table 3). Von Misses stress ranges from 1-9% approximately which is close to (Rivera et al., 2020) study whose results ranged from 1-7% compared to the Inventor® software. In any case, the trade-off for obtaining precise solutions in a short time offered by SimSolid® is a good alternative if you are looking to generate a large amount of data with CAE software.

6 CONCLUSIONS

Ti21S is a good alternative to Ti-6Al-4V, currently used in most stems. Although both materials are biocompatible due to their titanium content, aluminium in small quantities could produce toxicity effects when its debris enter the patient's bloodstream. The most notorious difference between both materials is Young's modulus, since the lower its value, the better, because it will more closely resemble the mechanical properties of the patient's cortical bone, producing a better load transfer and distribution. In this regard, Ti21S would be more likely to increase the implant's lifespan.

Currently, there is a growing demand for data in a short time for orthopaedic implants where the likelihood of successful outcomes and for a patient to acquire medical complications or pathologies (pneumonia, urinary tract infection, etc.) are

influenced by the preoperative time. Therefore, more research should be done on computational tools such as SimSolid®, which with a validated good accuracy could help to speed up the data acquisition process. Likewise, it can be complemented with ML-based models to extract local information from the femur and improve the process of prosthetic design customization.

Due to the complex morphology of the proximal femur, it is reasonable that deviations in results from simulations are greater than in the literature reviewed about SimSolid®, where common geometries, such as bars, cylinders, or spheres, were analysed. Furthermore, since these are approximate solutions, there will always be a simulation error, even between different FEA software working with conventional finite elements.

Although recently there has been extensive research on the design of short stem prostheses, studies on conventional cemented stems should not be neglected since they present better fixation in older adults and accelerate postoperative recovery. In addition, conventional prostheses are usually used in revision surgery, where short anterior stems help guarantee success, leaving sufficient good-quality bone stock improving the fixation of the new implant.

ACKNOWLEDGEMENTS

This work was funded by CONCYTEC-PROCIENCIA under the financial scheme "Becas de Mentorías María Reiche 2021-01" [Contract N°E053-2021-PROCIENCIA].

The authors express their gratitude to the Biomechanics Group of the Universidad de Piura for all their support in the development of this research. The authors acknowledge the support of reviewers and their relevant questions, which led to a more detailed and consistent paper.

REFERENCES

- Aherwar, A., Singh, A. K., & Patnaik, A. (2016). Cobalt based alloy: A better choice biomaterial for hip implants. *Trends Biomaterials and Artificial Organs*, 30(1), 50–55.
- Altair. (2019). *Simulation-Driven Design: Solving the Geometry Problem*.
- Amstutz, H. C., & Duff, M. J. Le. (2015). Hip resurfacing: history, current status, and future. *Wichtig Publishing*, 25(4), 330–338. <https://doi.org/10.5301/hipint.5000268>
- Arabnejad, S., Johnston, B., Tanzer, M., & Pasini, D. (2017). Fully porous 3D printed titanium femoral stem to reduce stress-shielding following total hip arthroplasty. *Journal of Orthopaedic Research*, 35(8), 1774–1783. <https://doi.org/10.1002/jor.23445>
- Barrack, R. L. (2000). Early failure of modern cemented stems. *Journal of Arthroplasty*, 15(8), 1036–1050. <https://doi.org/10.1054/arth.2000.16498>
- Bermejillo, M., Franco-Martínez, F., & Díaz, A. (2021). Artificial intelligence aided design of tissue engineering scaffolds employing virtual tomography and 3D Convolutional Neural Networks. *Materials*, 14(5278). <https://doi.org/https://doi.org/10.3390/ma14185278>
- Busch, V., Klarenbeek, R., Slooff, T., Schreurs, B. W., & Gardeniers, J. (2010). Cemented hip designs are a reasonable option in young patients. *Clinical Orthopaedics and Related Research*, 468(12), 3214–3220. <https://doi.org/10.1007/s11999-010-1355-z>
- Camacho, J., & Fernandez, J. (2006). Sir John Charnley (1911-1982). *Sociedad Mexicana de Ortopedia, AC*, 20.
- Chanda, S., Gupta, S., & Pratihari, D. K. (2015). A combined neural network and genetic algorithm based approach for optimally designed femoral implant having improved primary stability. *Applied Soft Computing Journal*, 38, 296–307. <https://doi.org/10.1016/j.asoc.2015.10.020>
- Chanda, S., Mukherjee, K., Gupta, S., & Pratihari, D. K. (2020). A comparative assessment of two designs of hip stem using rule-based simulation of combined osseointegration and remodelling. *Proceedings of the Institution of Mechanical Engineers, Part H: Journal of Engineering in Medicine*, 234(1), 118–128. <https://doi.org/10.1177/0954411919890998>
- Chatterjee, S., Dey, S., Majumder, S., RoyChowdhury, A., & Datta, S. (2019). Computational intelligence based design of implant for varying bone conditions. *International Journal for Numerical Methods in Biomedical Engineering*, 35(6), 1–17. <https://doi.org/10.1002/cnm.3191>
- Cilla, M., Borgiani, E., Martínez, J., Duda, G. N., & Checa, S. (2017). Machine learning techniques for the optimization of joint replacements: Application to a short-stem hip implant. *PLoS ONE*, 12(9), 1–16. <https://doi.org/10.1371/journal.pone.0183755>
- Cotogno, G. (2012). *Total hip arthroplasty: State of the art, prospects and challenges* (Issue July). Joint Research Centre of the European Commission. <https://doi.org/10.2788/31286>
- Eltit, F., Wang, Q., & Wang, R. (2019). Mechanisms of Adverse Local Tissue Reactions to Hip Implants. *Front. Bioeng. Biotechnol*, 7, 176. <https://doi.org/10.3389/fbioe.2019.00176>
- Facchini, L., Magalini, E., Robotti, P., Molinari, A., Höges, S., & Wissenbach, K. (2011). Ductility of a Ti-6Al-4V alloy produced by selective laser melting of prealloyed powders. *Rapid Prototyping Journal*. <https://doi.org/10.1108/13552541011083371>

- Gallart, X., Riba, J., Bori, G., Mu, E., & Combalia, A. (2018). Hip prostheses in young adults . Surface prostheses and short-stem prostheses. *Revista Española de Cirugía Ortopédica y Traumatología*, 62(2), 142–152.
- Gombár, C., Janositz, G., Frieber, G., & Sisák, K. (2019). The DePuy Proxima™ short stem for total hip arthroplasty – Excellent outcome at a minimum of 7 years. *Journal of Orthopaedic Surgery*, 27(2), 1–6. <https://doi.org/10.1177/2309499019838668>
- Gómez-García, F., Fernández-Fairen, M., & Espinosa-mendoza, R. (2016). A proposal for the study of cementless short-stem hip prostheses. *Acta Ortopédica Mexicana*, 30(4), 204–215.
- Hanada, S., Masahashi, N., Jung, T., & Yamada, N. (2014). Fabrication of a high-performance hip prosthetic stem using β Ti–33 . 6Nb–4Sn. *Journal of the Mechanical Behavior of Biomedical Materials*, 30, 140–149. <https://doi.org/10.1016/j.jmbbm.2013.11.002>
- Hu, C. Y., & Yoon, T. R. (2018). Recent updates for biomaterials used in total hip arthroplasty. *Biomaterials Research*, 22(1), 1–12. <https://doi.org/10.1186/s40824-018-0144-8>
- Jasty, M., Krushell, R., Zalenski, E., Connor, D. O., Sedlacek, R., & Harris, W. (1993). *The contribution of the nonporous distal stem to the stability of proximally porous-coated canine femoral components*. 8(1), 33–41.
- Javed, F., Ahmed, H., Crespi, R., & Romanos, G. (2013). Role of primary stability for successful osseointegration of dental implants: Factors of influence and evaluation. *Interventional Medicine and Applied Science*, 5(4), 162–167. <https://doi.org/10.1556/IMAS.5.2013.4.3>
- Jung, J. M., & Kim, C. S. (2014). Analysis of stress distribution around total hip stems custom-designed for the standardized Asian femur configuration. *Biotechnology and Biotechnological Equipment*, 28(3), 525–532. <https://doi.org/10.1080/13102818.2014.928450>
- Kang, Y. J., Yoo, J. Il, Cha, Y. H., Park, C. H., & Kim, J. T. (2020). Machine learning–based identification of hip arthroplasty designs. *Journal of Orthopaedic Translation*, 21, 13–17. <https://doi.org/10.1016/j.jot.2019.11.004>
- Katoozian, H., Devy, D. T., Arshi, A., & Saadati, U. (2001). Material optimization of femoral component of total hip prosthesis using fiber reinforced polymeric composites. *Medical Engineering & Physics*, 4533(October), 0–9. [https://doi.org/10.1016/S1350-4533\(01\)00079-0](https://doi.org/10.1016/S1350-4533(01)00079-0)
- Khanuja, H. S., Banerjee, S., Orth, M. S., Glasg, M., Jain, D., & Orth, M. S. (2014). Short Bone-Conserving Stems in Cementless Hip Arthroplasty. *Bone & Joint Surgery*, 96-A, 1742–1752.
- Kheir, M. M., Drayer, N. J., & Chen, A. F. (2020). An Update on Cementless Femoral Fixation in Total Hip Arthroplasty. *Journal of Bone and Joint Surgery*, 1646–1661.
- Kim, Y., Park, J., & Kim, J. (2013). Is Diaphyseal Stem Fixation Necessary for Primary Total Hip Arthroplasty in Patients with Osteoporotic Bone (Class C Bone)? *Journal of Arthroplasty*, 28(1), 139–146.e1. <https://doi.org/10.1016/j.arth.2012.04.002>
- Kuiper, J. H., & Huiskes, R. (1996). Friction and stem stiffness affect dynamic interface motion in Total Hip Replacement. *Journal of Orthopaedic Research*, 14, 36–43.
- Kunii, T., Mori, Y., Tanaka, H., Kogure, A., Kamimura, M., Mori, N., Hanada, S., Masahashi, N., & Itoi, E. (2019). Improved Osseointegration of a TiNbSn Alloy with a Low Young’s Modulus Treated with Anodic Oxidation. *Scientific Reports*, 9(1), 1–10. <https://doi.org/10.1038/s41598-019-50581-7>
- Kurtz, S. M., Ms, E. L., Ong, K., Ma, K. Z., Kelly, M., & Bozic, K. J. (2010). Future young patient demand for primary and revision joint replacement: National projections from 2010 to 2030. *Clinical Orthopaedics and Related Research*, 2009, 2606–2612. <https://doi.org/10.1007/s11999-009-0834-6>
- Learmonth, I. D., Young, C., & Rorabeck, C. (2007). The operation of the century: total hip replacement. *Lancet*, 370(9597), 1508–1519. [https://doi.org/10.1016/S0140-6736\(07\)60457-7](https://doi.org/10.1016/S0140-6736(07)60457-7)
- Nazari-farsani, S. (2015). *Precision and Accuracy of Marker-Based and Model-Based Radiostereometric Analyses in Determination of Three-Dimensional Micromotion of a Novel Hip Stem* (Issue December). Åbo Akademi University.
- Ojeda, C. (2009). Estudio de la influencia de estabilidad primaria en el diseño de vástagos de prótesis femorales personalizadas: aplicación aplicación a paciente específico. In *Tesis doctoral, Universidad Politécnica de Madrid*.
- Otomaru, I., Nakamoto, M., Kagiya, Y., Takao, M., Sugano, N., Tomiyama, N., Tada, Y., & Sato, Y. (2012). Automated preoperative planning of femoral stem in total hip arthroplasty from 3D CT data: Atlas-based approach and comparative study. *Medical Image Analysis*, 16(2), 415–426. <https://doi.org/10.1016/j.media.2011.10.005>
- Pellizzari, M., Jam, A., Tschon, M., Fini, M., Lora, C., & Benedetti, M. (2020). A 3D-Printed Ultra-Low Young’s Modulus β -Ti Alloy for Biomedical Applications. *Materials*, 1–16.
- Portal-Núñez, S., Lozano, D., De la Fuente, M., & Esbrit, P. (2012). Fisiopatología del envejecimiento óseo. *Revista Española de Geriatria y Gerontología*, 47(3), 125–131. <https://doi.org/10.1016/j.regg.2011.09.003>
- Rawal, B. R., Ribeiro, R., Malhotra, R., & Bhatnagar, N. (2011). Design and manufacture of short stemless femoral hip implant based on CT images. *Journal of Medicine on Science*, 11(8), 296–301.
- Raymond, D. (2019, June 28). *FemurFracture - Lower Extremity CTs*. Embodi3D.Com. <https://www.embodi3d.com/files/file/25956-femurfracture/>
- Rieker, C. B. (2016). Tribology of total hip arthroplasty prostheses. *EFORT Open Reviews*, 1(2), 52–57. <https://doi.org/10.1302/2058-5241.1.000004>
- Rivera, A. F., Castro, F. De, Moreno, A., & Rubio, J. C. (2020). Assessment of the Highest Stress Concentration

- Area Generated on the Mandibular Structure Using Meshless Finite Elements Analysis. *Bioengineering*, 1–11.
- Ruben, R. B., Fernandes, P. R., & Folgado, J. (2012). On the optimal shape of hip implants. *Journal of Biomechanics*, 45(2), 239–246. <https://doi.org/10.1016/j.jbiomech.2011.10.038>
- Ruben, R. B., Folgado, J., & Fernandes, P. R. (2007). A Three-Dimensional Model for Shape Optimization of Hip Prostheses Using a Three-dimensional shape optimization of hip prostheses using a multicriteria formulation. *Springer-Verlag Berlin Heidelberg, September*. <https://doi.org/10.1007/s00158-006-0072-4>
- Santori, F. S., Learmonth, I., Grifka, J., Valverde, C., & Kim, Y. H. (2007). *DePuy PROXIMA Hip - Surgical Technique*.
- Schaaff, P. (2004). The role of fretting damage in total hip arthroplasty with modular design hip joints - evaluation of retrieval studies and experimental simulation methods. *Journal of Applied Biomaterials & Biomechanics*, 2, 121–135.
- Schileo, E., Taddei, F., Cristofolini, L., & Viceconti, M. (2008). Subject-specific finite element models implementing a maximum principal strain criterion are able to estimate failure risk and fracture location on human femurs tested in vitro. *Journal of Biomechanics*, 41(2), 356–367. <https://doi.org/10.1016/j.jbiomech.2007.09.009>
- Schmitz, M. W., Busch, V. J., Gardeniers, J. W., Hendriks, J. C., Veth, R. P., & Schreurs, B. W. (2013). Long-term results of cemented total hip arthroplasty in patients younger than 30 years and the outcome of subsequent revisions. *BMC Musculoskeletal Disorders*, 14. <https://doi.org/10.1186/1471-2474-14-37>
- SimSolid Corporation. (2015). *SimSolid Technology Overview* (pp. 1–33).
- Sivasankar, D. M., Arunkumar, S., Bakkiyaraj, V., Muruganandam, A., & Sathishkumar, S. (2016). A Review on Total Hip Replacement. *International Research Journal In Advanced Engineering and Technology (IRJAET)*, 2(April), 589–642. <https://doi.org/10.13140/RG.2.2.13686.80969>
- Sköldenberg, O. G., Bodén, H. S. G., Salemyr, M. O. F., Ahl, T. E., & Adolphson, P. Y. (2006). Periprosthetic proximal bone loss after uncemented hip arthroplasty is related to stem size DXA measurements in 138 patients followed for 2 – 7 years. *Acta Orthopaedica*, 77(3), 386–392. <https://doi.org/10.1080/17453670610046307>
- Solórzano, W. (2021). *Innovación en el diseño personalizado de vástagos femorales cortos*. Universidad de Piura.
- Solórzano, W., Ojeda, C., & Lantada, A. D. (2020). Biomechanical study of proximal femur for designing stems for total hip replacement. *Applied Sciences (Switzerland)*, 10(12), 1–17. <https://doi.org/10.3390/APP10124208>
- Srinivasan, A., Jung, E., & Levine, B. R. (2012). Modularity of the Femoral Component in Total Hip Arthroplasty. *Journal of the American Academy of Orthopaedic Surgeons*, 20, 214–222.
- Subramanian, P., Wainwright, T. W., Bahadori, S., & Middleton, R. G. (2019). A review of the evolution of robotic-assisted total hip arthroplasty. *HIP International*, 29(3), 232–238. <https://doi.org/10.1177/1120700019828286>
- Sugano, N. (2013). Computer-assisted orthopaedic surgery and robotic surgery in total hip arthroplasty. *Clinics in Orthopedic Surgery*, 5(1), 1–9. <https://doi.org/10.4055/cios.2013.5.1.1>
- Symington, I. (2020). Designer Oriented Software - Is it Accurate? *The International Magazine for Engineering Designers & Analysts from NAFEMS, The Electromagnetics Issue*, 32–44.
- Wroblewski, B. M. (1997). Wear of the high-density polyethylene socket in total hip arthroplasty and its role in endosteal captation. *Proceedings of the Institution of Mechanical Engineers, Part H: Journal of Engineering in Medicine*, 211(1), 109–118. <https://doi.org/10.1243/0954411971534737>
- Yamako, G., Chosa, E., Totoribe, K., Hanada, S., Masahashi, N., Yamada, N., & Itoi, E. (2014). In-vitro biomechanical evaluation of stress shielding and initial stability of a low-modulus hip stem made of Beta type Ti-33.6Nb-4Sn alloy. *Medical Engineering and Physics*, 36(12), 1665–1671. <https://doi.org/10.1016/j.medengphy.2014.09.002>
- Yamako, G., Janssen, D., Hanada, S., Anijs, T., Ochiai, K., Totoribe, K., Chosa, E., & Verdonshot, N. (2017). Improving stress shielding following total hip arthroplasty by using a femoral stem made of β type Ti-33.6Nb-4Sn with a Young's modulus gradation. *Journal of Biomechanics*, 63, 135–143. <https://doi.org/10.1016/j.jbiomech.2017.08.017>
- Yan, S. G., Chevalier, Y., Liu, F., Hua, X., Schreiner, A., Jansson, V., & Schmidutz, F. (2020). Metaphyseal anchoring short stem hip arthroplasty provides a more physiological load transfer: a comparative finite element analysis study. *Journal of Orthopaedic Surgery and Research*, 15(1), 1–10. <https://doi.org/10.1186/s13018-020-02027-4>